



Full Length Article

Optimization of hydrocarbon water alternating gas in the Norne field: Application of evolutionary algorithms

Erfan Mohagheghian^a, Lesley A. James^{a,*}, Ronald D. Haynes^b

^a Faculty of Engineering and Applied Science, Memorial University of Newfoundland, St. John's, NL A1B3X5, Canada

^b Department of Mathematics and Statistics, Memorial University of Newfoundland, St. John's, NL A1C5S7, Canada



ARTICLE INFO

Keywords:

WAG optimization

Genetic algorithm

Particle swarm optimization

Net present value

Incremental recovery factor

ABSTRACT

Water alternating gas (WAG) is an enhanced oil recovery (EOR) method integrating the improved macroscopic sweep of water flooding with the increased microscopic displacement of gas injection. The optimal design of the WAG operating parameters is usually based on numerical reservoir simulation via trial and error. In this study, robust evolutionary algorithms are utilized to automatically optimize hydrocarbon WAG performance in the E-segment of the Norne field. Net present value (NPV) and two global semi-random search strategies, a genetic algorithm (GA) and particle swarm optimization (PSO), are used to optimize over an increasing number of operating parameters. The operating parameters include water and gas injection rates, bottom-hole pressures of the oil production wells, cycle ratio, cycle time, the composition of the injected hydrocarbon gas and the total WAG period. In progressive case studies, the number of decision-making variables is increased, increasing the problem complexity while potentially improving the efficacy of the WAG process. We also optimize the incremental recovery factor (IRF) within a fixed total WAG simulation time. The distinctions between the WAG parameters found by optimizing NPV and oil recovery are highlighted. This is the first known work to optimize over such a wide set of WAG variables and the first use of PSO to optimize a WAG project at the field scale. Compared to the reference cases, the best overall values of the objective functions found by GA and PSO were 13.8% and 14.2% higher, respectively, if NPV is optimized over all the above WAG operating variables, and 14.2% and 16.2% higher, respectively, if the IRF is optimized.

1. Introduction

Enhanced oil recovery (EOR) techniques are meant to decrease the residual oil saturation after primary and secondary oil production [1]. Gas injection as an EOR process is widely used for increasing oil recovery by injecting gases into the oil reservoir [1–6]. A low mobility ratio between the injected gas and the displaced oil during the immiscible displacement process leads to an unstable zone on the front as well as early breakthrough and viscous fingering [7,8]. Water alternating gas (WAG) was first proposed as a method to integrate the improved microscopic displacement efficiency of gas injection with the increased macroscopic sweep efficiency of water flooding [9].

WAG has been conducted with success in most field trials. The majority of the fields subjected to WAG are located in Canada and the United States. WAG incremental oil recovery is reported to be about 5%, however, incremental recovery has reached up to 20% in several fields. High incremental recovery is usually a result of the gas being miscible with the reservoir oil. Carbon dioxide (CO₂) and hydrocarbon gases are the two most commonly used injectants. CO₂ is expensive, not

easily available, especially for offshore purposes, and it can cause corrosion issues [10,11], however, hydrocarbon gases are directly obtained from oil production or from a nearby gas field, and in almost all offshore WAG applications hydrocarbon gases are injected either as dry gas or are enriched before injection [9].

It is crucial to develop and test various WAG scenarios in order to determine the optimum operational parameters based on economics [12]. Parameters which can affect WAG are classified into reservoir characteristics (such as heterogeneity, wettability, fluid properties) and operational/well control parameters (injection pattern, injection rates, bottom-hole pressures of the oil producers, WAG or cycle ratio, cycle time, the composition of the injection gas and the total WAG duration) [9,13–17]. Reservoir characteristics are usually either uncontrollable or too costly to modify, hence locating the optimal operational point is of vital significance. Non-optimal well control parameters are likely to result in early breakthrough and high water cut and/or gas-oil ratio, thus low oil recovery and less profit. To the best of the authors' knowledge, no automatic optimization has ever been done on the whole set of control variables prepared here. As the number of controlling

* Corresponding author.

E-mail address: ljames@mun.ca (L.A. James).

variables increases, the optimization of WAG performance in a heterogeneous reservoir becomes more complex and challenging.

Several previous simulation studies have used a limited number of runs and suggested field performance surveillance to optimize WAG parameters [12,18–21]. Ampomah et al. optimized WAG cycles using numerical reservoir simulators and proposed longer gas cycles to increase oil recovery and CO₂ storage [22]. Gharbi utilized an expert system, as a subclass of Artificial Intelligence, combined with an economic package, to optimize WAG ratio, slug size per WAG cycle and then the total slug size by changing the variables incrementally in small ranges [23]. Esmaili and Heeremans, Ghomian et al., and Ghaderi et al. used response surfaces as a proxy for the reservoir simulator to optimize the WAG parameters by means of a polynomial expression [24–26]. Dai et al. [27,28] employed a response surface analysis and Monte Carlo simulation to optimize a CO₂-EOR process and found the optimal distance between the wells and the sequence of alternating injection cycles. Rahmawati et al. solved the mixed-integer nonlinear optimization problem for different flooding strategies and employed a heuristic simplex algorithm to find the maximum NPV and the best injection scenario. They mentioned that the NPV should be tested and maximized for the optimum field production life time (before the negative return of NPV) [29]. Jahangiri used Ensemble Kalman filter (EnKF) to optimize the net present value of a WAG process by controlling the injection rates, bottom hole pressures of the producers and injection pattern as the variables. He showed the flexibility of EnKF in the choice of simulator and economic model and its low computational cost [30].

Yang et al. used a genetic algorithm (GA) and simulated annealing to optimize the multivariate production-injection system for WAG miscible flooding using net present value as the objective function. They chose average reservoir pressure, producing GOR, water-cut and oil rate for each production well, and gas or water injection volume as the decision-making variables. They claimed that both of the techniques showed stability and efficiency for their optimization purpose [31,32]. Chen et al. used a GA to optimize the controlling variables (WAG ratio, cycle time, injection rates and bottom hole pressures of the producers) of a CO₂-miscible WAG in field scale. They hybridized the GA with an orthogonal array and Tabu search to improve the convergence speed of GA [14]. However, they limited all the optimization variables to take only a few discrete values.

The huge number of alternative WAG control schemes necessitates the employment of efficient and robust optimization algorithms to make the most profitable decision. We use a genetic algorithm (GA) and particle swarm optimization (PSO) in this study. GA has gained much popularity in the petroleum industry and both of these techniques have proven their capability in finding the optima of various oil and gas problems [33–35]. These are black-box algorithms which do not need access to the simulator code and can be efficiently parallelized. GA has already been used for the purpose of WAG optimization, however, the injection gas composition was not included and the number of variables was lower than those optimized in this paper. PSO is tested here to optimize a WAG project in the field scale for the first time.

In this study, D-optimal design, a design of experiments (DOE) approach which spans the whole search space more efficiently than a full factorial design [36], is integrated with GA and PSO to improve the initialization process of the algorithms and is also used as the reference case to monitor the success of our optimization. NPV and incremental recovery factor (IRF) are selected as objective functions and the set of controllable operating parameters include water and gas injection rates, bottom-hole pressures of the oil producers, cycle ratio, cycle time, the composition of the injected hydrocarbon gas and the total WAG period. Three case studies on NPV optimization and one on IRF optimization are designed. The case studies are carried out on the E-segment of the Norne field (See Section 3 for more information on the field). In progressive case studies, an incremental number of variables are sampled from this set to examine the practicality of the optimization algorithms and the increased efficacy of the WAG process as the problem

complexity increases. We show that such optimization techniques will succeed at finding the optimal solution and increase the economic benefit.

2. Methodology

In this section, the objective functions, well control parameters (optimization variables), optimization techniques and the optimization procedure used in this study are explained and illustrated.

2.1. Objective functions

In production optimization, the ultimate recovery factor or net present value (NPV) is usually chosen as the objective (fitness) function. Although NPV, as an economic measure, is not the only influencing factor, it is a proper indication of the project's profitability and helps in decision making. NPV is defined as the sum of the present values of incoming and outgoing cash flows over a period of time [14]. NPV for a WAG process can be calculated as

$$NPV(x) = \sum_{i=1}^n \{Q_o^{prod}(i)c_o - [Q_g^{inj}(i) - Q_g^{prod}(i-1)]c_g - Q_g^{prod}(i-1)c'_g \dots \\ - [Q_w^{inj}(i) - Q_w^{prod}(i-1)]c_w - Q_w^{prod}(i-1)c'_w\}(1+r)^{-i} \dots \\ + [Q_g^{prod}(n)(c_g - c'_g) + Q_w^{prod}(n)(c_w - c'_w)](1+r)^{-n}, \quad (1)$$

where n is the total number of years, i is the year number, c_o is the price of produced oil, c_g and c_w are the price for purchasing gas and water for injection, c'_g and c'_w are the cost of treating and recycling the produced gas and water, Q is the total volume of the produced or injected fluid and r is the interest rate. The subscripts o, w and g refer to oil, water and gas and the superscripts inj and $prod$ represent injection and production, respectively. The volumes are obtained as outputs of the reservoir simulator and are functions of the optimization vector x .

The total oil production after the start of the WAG divided by the initial oil in place, known as incremental recovery factor (IRF), is the second objective function used in this study. IRF is defined in the following form

$$IRF = \frac{\int_0^T q_o dt}{IOIP}, \quad (2)$$

where T is the total WAG duration, q_o is the total oil production rate and $IOIP$ is the initial oil in place.

2.2. Well control parameters

The three subsystems, namely reservoir, well and surface facilities are often treated independently and the locally optimized results of each subsystem is handed off to its next downstream stage for functional analysis [37]. It is important to consider the problem of production optimization as an integrated system and optimize the subsystems' performance globally. Therefore, in this paper both the injection and production parameters are taken into account.

Due to reservoir heterogeneity, different injection rates/flowing bottom hole pressures are assigned to each injector/producer. Injection rates should be chosen according to fracturing pressure and well injectivity and the producers' bottom-hole pressures (BHPs) should vary in a range which conforms to well and surface facility constraints. It is economical to maintain the BHP at, or close to, the minimum miscibility pressure (MMP) if sufficient drawdown can be applied in the reservoir [14].

Other WAG injection parameters include the length of a period of water and gas injection. This is known as the cycle time. Another WAG injection parameter requiring investigation is the ratio of water to gas injection which can be defined by WAG ratio or cycle ratio. WAG ratio is the ratio of the volume of water to the volume of gas injected at

reservoir conditions and cycle ratio is the ratio of water injection time to the total cycle time. Cycle time varies the number of cycles in a fixed total production time, and hence affects ultimate recovery. Higher WAG or cycle ratio results in more favorable mobility, whereas a lower ratio diminishes the residual oil saturation and extends the waterless production period [13]. Therefore, the optimal cycle time and ratio should be carefully determined to improve the efficiency of WAG process. While the total time of a WAG process is usually fixed, we include it as one of the optimization variables in this study due to the uncertainties in reservoir life predictions and the negative return of accumulated NPV versus time.

Another parameter which is rarely optimized is the injection gas composition. It is essential to study the effect of gas composition on the miscibility in the course of design and optimization of a gas flooding project [38]. It would be economical to make the injection miscible by altering the composition if the increase in oil recovery could justify the costs of gas enrichment.

2.3. Optimization techniques

Due to the complexities of WAG optimization in field scale and intricacies of relations between the objective function and the decision-making variables, efficient and robust optimization methods are required to obtain the most economical WAG control parameters. Both GA and PSO are heuristic global stochastic search algorithms which have demonstrated their competence in solving optimization problems. D-optimal design is used to help initialize the searching procedure and improve the convergence speed. All the simulation runs during the optimization search are stored, so redundant runs are avoided and parallel computation is utilized to save computational time. We now briefly present an overview of the optimization methods used in this paper.

2.4. Genetic algorithm

In 1975, Holland proposed genetic algorithms “as an abstraction of biological evolution” [39]. Over the last 20 years, this algorithm has attracted much attention from various fields as an optimization technique to solve complex and nonlinear problems [40]. This algorithm is recognized as an efficient, robust, parallel, and global randomized searching algorithm which copes with a given problem by investigating and exploiting the search space, and solves the problem by using a set of encoded variable strings, which are called chromosomes. To conduct its optimization process, GA evolves its population from one generation (parents) to the next (offspring) by means of the operations of selection, mutation and crossover [41].

The parents are selected randomly through the selection process and chromosomes with higher fitness values are more likely to be chosen. In the crossover operation, two parent chromosomes are combined and part of their genetic information is exchanged to produce the offspring. Before inserting the offspring with the best fitness values back into the original population, a mutation operator causes the GA method to span the search space more thoroughly and introduce variety in the population. It is expected that GA obtains the optimal solution through the combination of these three steps, however convergence is not guaranteed [41]. GA has been used in the oil industry more than other evolutionary algorithms [42].

In this study, the “stochastic uniform” method is used for selection. Parents are selected at a rate which is randomly proportional to their scaled values. An elite count of 2 with a scattered crossover fraction of 0.8 and uniform mutation rate of 0.01 are used [43]. A population size of 50 with 40 generations (total of 2000 simulation runs) are applied in each of the GA optimization trials.

2.5. Particle swarm optimization

In 1995, Eberhart and Kennedy introduced particle swarm optimization (PSO) which was inspired by the social behavior and movement dynamics of animals [44]. PSO is similar to GA, however, PSO uses the collaborative approach rather than the competitive one used in GA [45]. PSO uses a number of particles to span the search space. The position of particle i at iteration k , (x_i^k) , is a vector with dimension equal to the number of optimization variables. The particles form a population of random solutions and are stochastically distributed over the solution space. Each particle in the swarm potentially finds a solution to the optimization problem and moves towards the global optimum of the objective function. Each particle remembers its most recent position in the search space, its best ever position, (p_i^k) , and the swarm’s best ever global solution, (g_i^k) .

In the optimization process, the position of each particle in the next iteration is updated by

$$x_i^{(k+1)} = x_i^k + v_i^{(k+1)} \quad (3)$$

Each individual modifies its velocity to find the most promising solution based on the following relationship [46]

$$v_i^{(k+1)} = \omega v_i^k + C_1 r_1 \otimes (p_i^k - x_i^k) + C_2 r_2 \otimes (g_i^k - x_i^k), \quad (4)$$

where ω is the inertia weight and C_1 and C_2 are the cognitive and social learning coefficients, respectively. The quantities r_1 and r_2 represent two random parameters in the range of (0, 1) which are multiplied componentwise, via the operator \otimes , with the terms in the brackets.

The inertia weight as a linear function of the iteration index is represented by [46]

$$\omega = \omega_{\max} - \frac{(\omega_{\max} - \omega_{\min})}{k_{\max}} k, \quad (5)$$

where ω_{\max} expresses the maximum magnitude of the inertia weight, ω_{\min} is the minimum magnitude of the inertia weight, k represents the current iteration, and k_{\max} denotes the total number of iterations.

Perez and Behdinan [47] demonstrated that the particle swarm is only stable if the following conditions are satisfied

$$0 < C_1 + C_2 < 4, \quad (6)$$

$$\frac{C_1 + C_2}{2} - 1 < \omega < 1. \quad (7)$$

If the above conditions are met, PSO is guaranteed to converge to a stable equilibrium point. However, whether or not this point is actually the global optimum cannot be guaranteed. In this study, the parameter values of $C_1 = 0.5$, $C_2 = 1.25$, $\omega_{\max} = 0.9$ and $\omega_{\min} = 0.4$ were used. These parameter values have shown good convergence results in literature [48,49]. 50 particles and 40 iterations (totally 2000 simulation runs) are used in each of the PSO optimization trials in this study.

2.6. Optimization procedure

Fig. 1 shows the flowchart for model-based WAG optimization conducted in this study. The optimization is done on a fixed history matched reservoir model. After history matching, the best simulation runs from the results of DOE are used to initialize the search process. The variables (WAG injection/production parameters) are written in the suitable format in a file included in the main simulation data file and the compositional reservoir simulator (in this case Schlumberger’s Eclipse E300 [50]) is called to calculate the oil recovery and profiles of cumulative oil, gas and water for each point in the solution space (particle in PSO or individual in GA terminology). Cumulative oil production is calculated directly for the purpose of oil recovery optimization. NPV for each individual WAG scenario is computed using Eq. (1) as coded in the economic module. A stopping criterion (usually based on the computational budget or maximum CPU time) is defined.

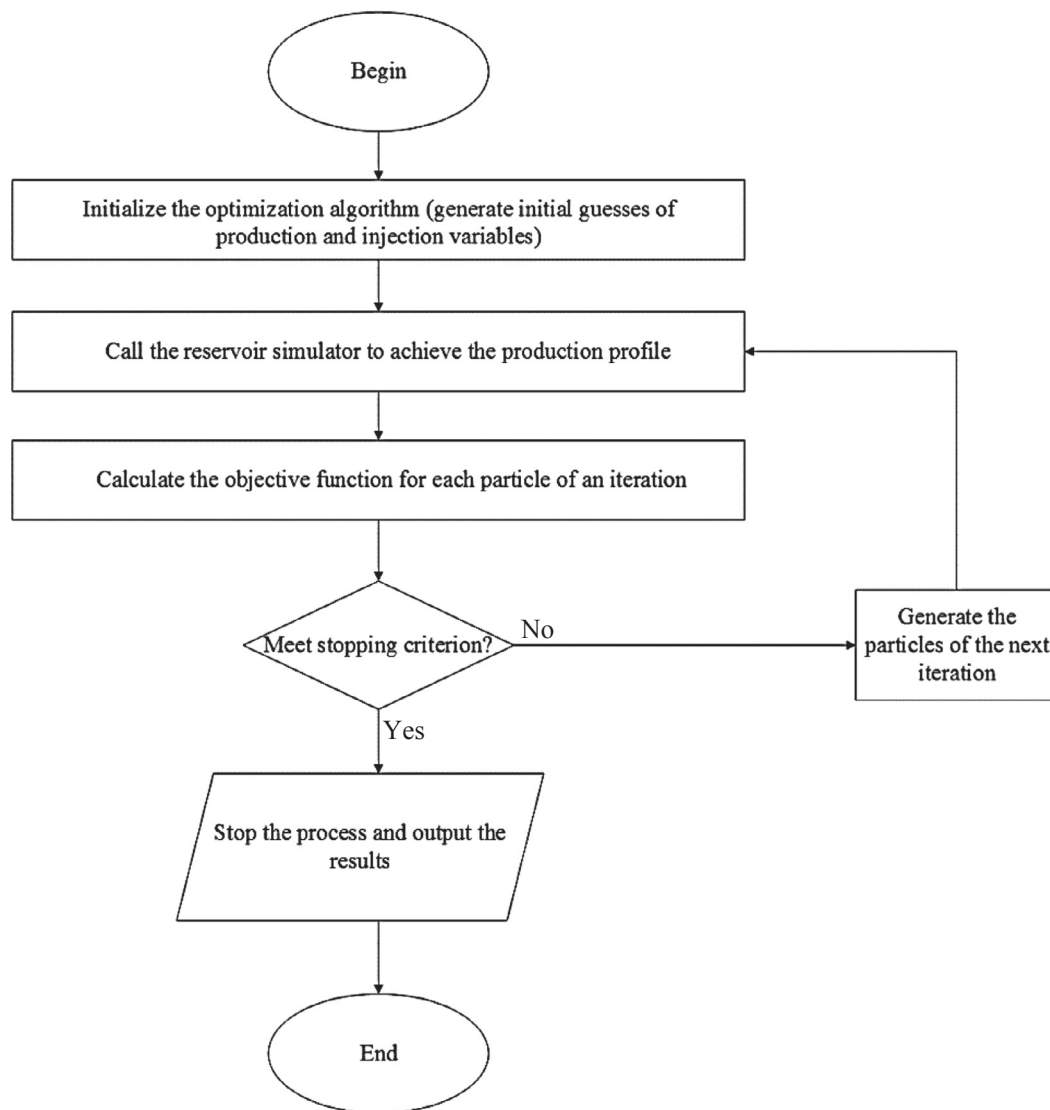


Fig. 1. Flowchart of the WAG optimization process.

GA generates the next population by means of selection, crossover and mutation operators and PSO updates the velocity and position of the particles using Eqs. (2) and (3). The aforementioned process is iterated until the stopping criterion is met. The stopping criterion here is a maximum limit on the number of iterations. Then the process is terminated and the results can be viewed. The whole optimization process is done automatically and without any manual interruption. Here we use a generic implementation of GA and PSO which have been shown to be robust for a large class of problems. Improvements of both optimization algorithms are likely possible by tuning for the specific problem of interest.

3. Field background

The Norne field dataset, including two case studies for the whole field and the E-segment, is hosted and supported by the Integrated Operations (IO) center at Norwegian University of Science and Technology (NTNU). The Norne field on the Norwegian Continental Shelf is operated by Statoil, a partner of the IO center. The Norne oil field was discovered in December 1991. It is located about 80 km north of the Heidrun field in the Norwegian Sea in about 380 m of water. Development drilling began in August 1996 and oil production started on November 6th 1997. The horst block is approximately 9 km × 3 km.

The Norne main structure (Norne C, D and E-segments) containing 97% of the oil in place, and the North-East Segment (Norne G-segment) are the two separate oil compartments of the field [51]. The oil bearing sandstones are buried at a depth of 2500–2700 m. The porosity is in the range of 25–30% and permeability varies from 20 to 2500 mD. The initial reservoir pressure was about 273 bar at 2639 m true vertical depth (TVD) and the reservoir temperature is 98.3 °C

The total hydrocarbon column is 135 m which contains 110 m of oil and 25 m of gas. Gas injection stopped in 2005 and the oil is produced with water injection as drive mechanism. The Norne field was expected to produce for 20–24 years with abandonment in 2020 [52]. However, Statoil has made an oil discovery in the Svale North prospect in the Norwegian Sea about 9 km northeast of the Norne field and is pushing operation until 2030 [53].

In this paper, we assume the E-segment is separated from the rest of the field. The E-segment contains 8733 active cells. The sizes of the blocks are between 80 m and 100 m in the horizontal direction. The rock is of mixed wettability and pore compressibility is $4.84 \times 10^{-5} \text{bar}^{-1}$ at 277 bar [54]. The E-segment of the Norne field with the active injectors (F-1H and F-3H) and producers (E-2AH, E-3CH and E-3H) in place, at the end of 2006, is shown in Fig. S1.

The reservoir fluid is characterized as light oil with a gravity of 32.7° API, bubble point pressure of 251 bar, gas-oil ratio of 111 Sm³/

Sm^3 , oil formation volume factor of 1.347 and $1.3185 \text{Rm}^3/\text{Sm}^3$ at bubble point and initial reservoir pressure, respectively, oil density and viscosity of $0.712 \text{g}/\text{cm}^3$ and 0.58cP at bubble point pressure and gas formation volume factor of $0.00474 \text{Rm}^3/\text{Sm}^3$ [55]. The detailed compositional analysis of the reservoir oil is presented in Table S1.

It is worth noting that all the simulation studies already done on the Norne field have been run in Black Oil mode [52,55–57]. The above composition and fluid properties data was regressed using PVTi module of Eclipse (version 2014.1) and E300 was utilized as the compositional reservoir simulator in this study. By doing so, the effect of injection gas composition on the objective function can be investigated. History matching was also conducted up to December 2006 (based on the available production and history data) to improve the accuracy of the model and reduce the simulations' uncertainty.

4. Case studies

Three case studies for optimization of NPV and one case study for optimization of IRF were designed in this study. The full set of optimization variables consists of two water and two gas injection rates for the two injectors, three BHPs of the three oil producers, cycle ratio, cycle time, the mole fractions of C_2 , C_3 and C_4 and the total WAG period (13 variables in total). The parameter values provided in Table S2 were used for NPV calculations in all the case studies.

Water flooding was performed on the model (history matched up to December 2006) with sufficiently low rates in the two injectors to reach the value of 90% for the field water cut in May 2015. This was considered as the initial point for WAG simulations and optimization.

There are two types of constraints in the optimization of an oil recovery process, namely general economic and bound constraints. The economic constraints consist of a lower limit on oil production ($10 \text{Sm}^3/\text{day}$) and upper limits on water cut (95%) and GOR (500 vol/vol) for all the production wells' perforations. If the upper limits are violated, the worst offending perforation will be shut and the simulation continues until at least one perforation is open. A maximum liquid production rate in each producer of $6000 \text{Sm}^3/\text{day}$ and a maximum injection pressure in each injector of 600 bar are also placed in the simulation data file. The bound constraints are of the simple inequality type as shown in Table 1. It is worth noting that only discrete values (with the specified step sizes) are assigned to the cycle ratio, cycle time and total WAG duration and the rest of the variables are assumed to be continuous.

GA and PSO handle bound constraints differently. In GA, mutation and crossover functions are defined to generate only feasible solutions [43]. In this study, the 'absorb' method was used for handling bound constraints in PSO so that the algorithm prevents the particles from traveling outside the bounds. This method has proven to be sufficiently efficient for problems which only include bound constraints [58].

In case study 1, two water and two gas injection rates, three BHPs of the production wells, cycle ratio and cycle time (nine variables) are optimized. The mole fractions of the injection gas components are fixed at their lower bounds. The gas injection is immiscible in this case since

Table 1
The optimization variables along with their ranges in this study.

Optimization variable	Range
Water injection rates [Sm^3/day]	500–2700
Gas injection rates [Sm^3/day]	10^3 – 10^6
Producers bottom hole pressures [bar]	150–240
Cycle ratio [–]	0–1 in steps of 0.05
Cycle time [month]	2–12 in steps of 1 month
Mole fraction of C_2 [–]	0.05–0.2
Mole fraction of C_3 [–]	0.02–0.1
Mole fraction of C_4 [–]	0.01–0.05
Total WAG duration [month]	30–60 in steps of 1 month

the MMP of the reservoir oil and injection gas is calculated to be about 550 bar using PVTsim software, which is far above the reservoir pressure. In case study 2, the injection gas composition (the mole fractions of C_2 , C_3 and C_4) are added to the optimization variables giving a total of 12 variables. The MMP between the reservoir oil and the most enriched gas is calculated to be about 330 bar, so miscibility could be achieved in the reservoir. In case studies 1 and 2, the total WAG simulation time is fixed at 30 months. We include the total WAG time as a variable in case study 3 where we optimize over all 13 variables. For the purpose of IRF optimization, only one case study is conducted with the 12 decision variables used in case study 2 and using a fixed total WAG simulation time of 60 months. The rationale behind the progressive case studies is to investigate the effect of increasing the number of variables on the optimal solution and to provide some information about the efficiency of the two optimization techniques.

In this study, D-optimal design was used to obtain the initial guess for the optimization algorithms. In case study 3, for example, a full factorial design requires 27,648 simulation runs. D-optimal design is able to search the solution space with only 110 runs. For case studies 1 and 2, with nine and 12 variables, respectively, D-optimal design only requires 60 and 96 simulation runs. For each case study, the best configurations found by DOE were used to initialize the population and particles for GA and PSO, respectively. This was done to improve the convergence speed of the optimization algorithms. The best WAG scheme among the initial guesses was also selected as the reference case to be compared with the optimization results.

Due to the stochastic nature of the optimization techniques, multiple trials are required for each case study. The compositional simulations are time consuming, so the objective function calculations are costly and demanding. We perform four trials with 2000 objective function evaluations using both GA and PSO (i.e., eight trials in total) for each of the three NPV optimization case studies; and three trials again with 2000 objective function evaluations using the same algorithms (i.e., six trials in total) for IRF optimization. Each objective function evaluation requires a reservoir simulation run. Each trial used 50 individuals or particles for 40 generations or iterations.

5. Results and discussion

In this section we present the results of case studies 1, 2 and 3 to optimize NPV and a single case study to optimize IRF using GA and PSO. Sensitivity studies are also conducted to investigate the effect of decision variables and economic parameters on NPV.

5.1. Case study 1: NPV optimization over 9 variables

In case study 1, two water and two gas injection rates, three BHPs of the oil producers, cycle ratio and cycle time are the nine optimization variables. The total WAG duration is fixed at 30 months and the mole fractions of C_2 , C_3 and C_4 are fixed at 0.05, 0.02 and 0.01, respectively. The top 50 results out of the 60 simulation runs from the DOE are used as the initial positions for the 50 particles in PSO and the 50 members of the population for the GA optimization and the best of the 50 is chosen as the reference case for comparison.

Table 2 shows the values of the decision variables and the NPV for the reference case and for the best overall solutions found by the optimization techniques. As can be seen, PSO located the same optimal solution in all of its four trials, while GA was able to arrive at the best answer found by PSO only once. The values of the optimized variables which differ from the reference case have been marked with an asterisk. The numerical results of the four trials of GA and PSO are tabulated and presented in Tables S3 and S4 respectively in the Supplementary document.

As indicated by asterisks in Table 2, one of the BHPs (well E-2AH) changed from 150 bar to 158.8 bar, the cycle ratio shifted from 0.65 to 0.9 and the cycle time changed from 4 months to 5 months in the

Table 2

The reference case and best operational points found by GA and PSO (case study 1: NPV optimization over 9 variables). * Optimized variables which differ from the reference case.

Variable	Reference case	GA trial 3	PSO trials 1–4
Q _w (F-1H) [Sm ³ /day]	2700	2700	2700
Q _g (F-1H) [Sm ³ /day]	1000	1000	1000
Q _w (F-3H) [Sm ³ /day]	2700	2700	2700
Q _g (F-3H) [Sm ³ /day]	1000	1000	1000
BHP (E-2AH) [bar]	150	158.8*	158.8*
BHP (E-3CH) [bar]	150	150	150
BHP (E-3H) [bar]	150	150	150
Cycle ratio [–]	0.65	0.9*	0.9*
Cycle time [month]	4	5*	5*
NPV [\$ million]	135.45	146.56	146.56

optimal configuration found by the algorithms. The overall optimal NPV is about 8.2% higher than the NPV of the initial reference case.

Fig. 2 depicts the best performance of the optimization techniques in the four trials. The best NPV found by the algorithms in each trial is displayed versus the iteration index for iterations 11–40. The plots of best NPV for all the iterations of the four trials of the algorithms can be viewed in the Supplementary file in Fig. S1. Fig. 2 shows that GA produces a non-decreasing NPV curve throughout its search; however, it usually converges to solutions which are marginally lower than those found by PSO. The version of PSO used in this study converges to the same optimal solution in its four trials, however, small fluctuations can be observed in the best NPV value versus PSO iteration index. GA finds a solution with an NPV in the vicinity of 0.01% of the optimum solution for the first time in iteration 9 of the third trial and fails to find such an answer in the other trials. PSO gives a solution in the specified range for the first time in iteration 7 of trials 1–3 and iteration 8 of trial 4. We see that generally the default optimization of PSO outperforms GA for this example.

5.2. Case study 2: NPV optimization over 12 variables

In case study 2, the injection gas composition (the mole fractions of

Table 3

The reference case and best operational points found by GA and PSO (case study 2: NPV optimization over 12 variables).

Variable	Reference case	GA trials 2, 3	PSO trials 1–4
Q _w (F-1H) [Sm ³ /day]	2700	2700	2700
Q _g (F-1H) [Sm ³ /day]	380,620	1000*	1000*
Q _w (F-3H) [Sm ³ /day]	2700	2700	2700
Q _g (F-3H) [Sm ³ /day]	1000	1000	1000
BHP (E-2AH) [bar]	150	158.9*	158.8*
BHP (E-3CH) [bar]	150	150	150
BHP (E-3H) [bar]	201.3	150*	150*
Cycle ratio [–]	0.7	0.9*	0.9*
Cycle time [month]	2	2	5*
Mole fraction of C ₂ [–]	0.05	0.2*	0.2*
Mole fraction of C ₃ [–]	0.1	0.1	0.1
Mole fraction of C ₄ [–]	0.05	0.05	0.05
NPV [\$ million]	132.09	148.66	148.76

C₂, C₃ and C₄) are added to the optimization variables of case study 1, giving 12 variables in total. The total WAG duration is fixed at 30 months. The top 50 results out of the 96 simulation runs from the DOE are used as the initial positions for the 50 particles in PSO and the 50 members of the population for the GA optimization and the best of the 50 is chosen as the reference case for comparison. The values of the decision variables and NPVs for the reference case and the best solutions located by the optimization algorithms are presented in Table 3. The values of the optimized variables which differ from the reference case have been marked with an asterisk. Tables S5 and S6 in the Supplementary file show the best overall solutions of all the individual trials of GA and PSO, respectively.

In this case, the reference solution has a lower NPV than that of case study 1. Here more simulation runs are conducted for the DOE than in case study 1 (96 compared to 60), however, DOE is not able to provide as good an initial guess. Case study 2 is more complex and has a higher dimensional search space (12 variables in case study 2 compared to nine variables in case study 1).

As shown in Table 3, PSO was able to reduce the gas injection rate of well F-1H to its minimum (1000 Sm³/day), increase the BHP of well E-

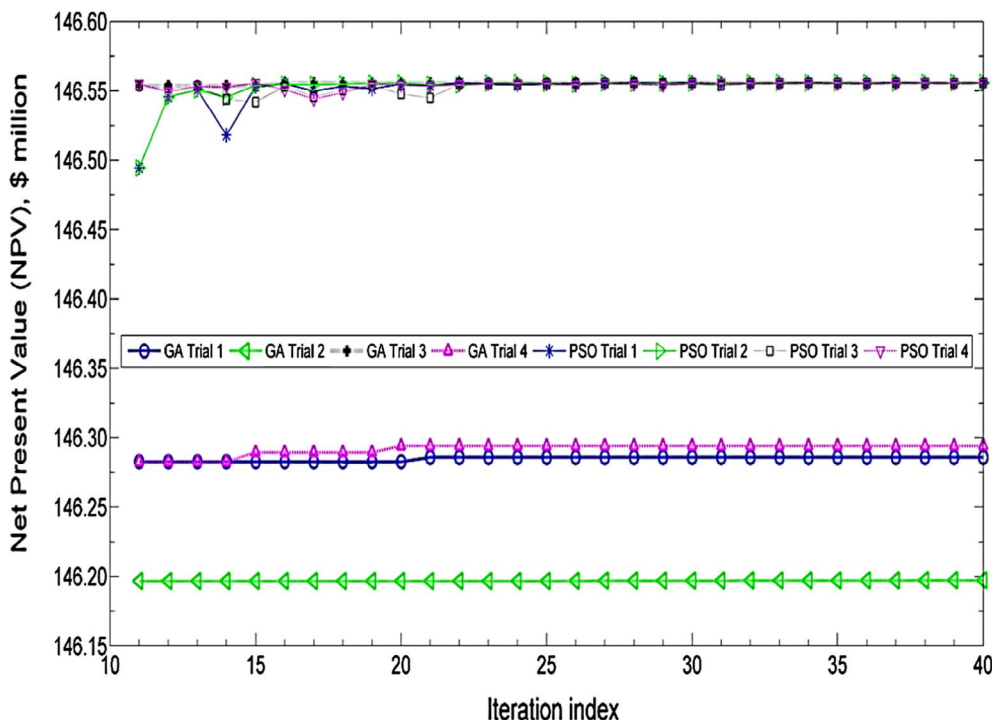


Fig. 2. NPV vs. iteration index per trial for iterations 11–40 of GA and PSO (case study 1: NPV optimization over 9 variables).

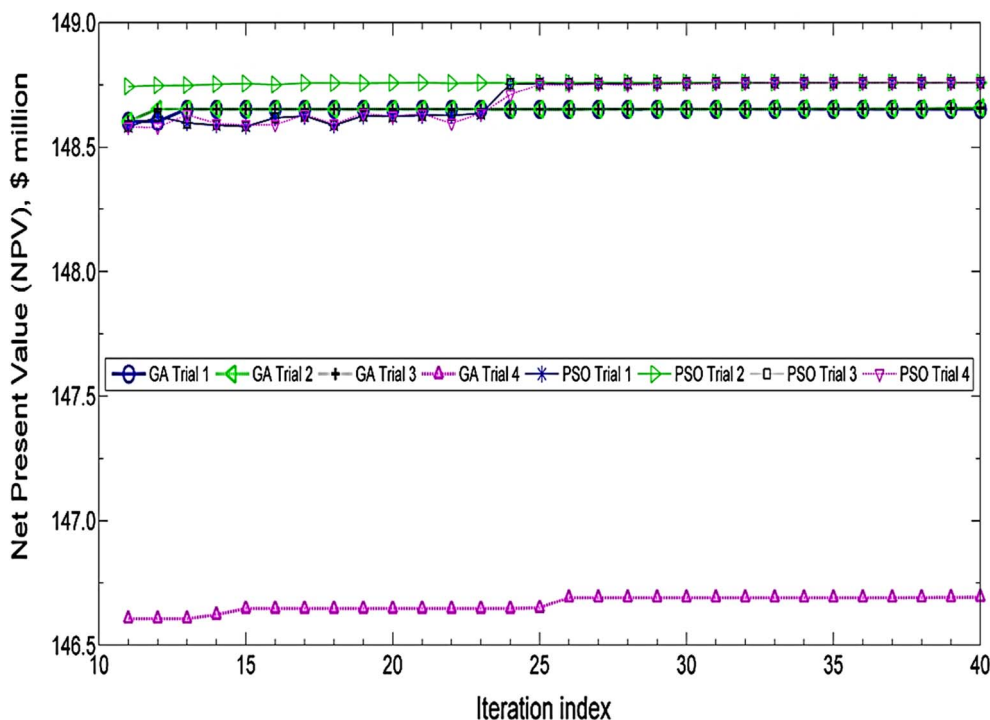


Fig. 3. NPV vs. iteration index per trial for iterations 11–40 of GA and PSO (case study 2: NPV optimization over 12 variables).

2AH from 150 to 158.8 bar and decrease the BHP of well E-3H to the minimum (150 bar), change the cycle ratio from 0.7 to 0.9 and increase the mole fraction of ethane in the injection gas from 0 to the maximum (0.2). The best overall NPVs found by GA and PSO are respectively about 12.5% and 12.6% higher compared to the NPV of the reference case. GA fails to change the cycle time in all the four trials and gets stuck at the value of the reference case. Unlike GA, PSO gives the same optimal solution in all the trials. However, the difference between the best answers found by GA and PSO is negligible and mainly due to the effect of different cycle times.

Fig. 3 displays the best NPVs found by GA and PSO for each trial versus the iteration index for iterations 11–40. Fig. S3 in the Supplementary file presents the results of all the iterations of the four trials of the algorithms. As depicted in Fig. 3, GA shows a monotonic trend and except in trial 4, it converges to approximately the same answer. PSO shows general superiority over GA and convergence to the same optimal solution in all the four trials in spite of minor fluctuations.

The optimal NPV found in the first trial of GA is a little lower than the best NPV found in trials 2 and 3. This is due to the higher value of BHP for well E-2AH (see Tables S5). In trial 4, GA changes the value of the gas injection rate of well F-1H and the BHP of well E-2AH to values which result in the lowest NPV of all the trials of the optimization techniques. In other words, GA has the poorest performance in trial 4.

The first nine variables of the optimal solution of case study 2 have the same values as those of case study 1, while a better NPV has been achieved due to enriching the gas and a more miscible injection which increases oil recovery. The optimal NPV of case study 2 is about 1.5% higher than the corresponding value for case study 1. So even though the reference case for case study 2 has a lower NPV compared to case study 1, the optimization techniques have been able to improve the optimal solution.

PSO finds a solution with an NPV in the vicinity of 0.01% of the optimal solution for the first time in iteration 24, 7, 24 and 25 of trials 1–4, respectively. GA fails to achieve such a solution. Compared to case study 1, a poorer initial guess definitely influences the number of iterations required to find a solution close to the optimal solution, hence the effect of problem complexity by adding more variables is

difficult to discern.

5.3. Case study 3: NPV optimization over 13 variables

In case study 3, the total WAG period is added to the optimization variables of case study 2. This gives 13 variables in total. The initial positions for GA and PSO and the reference case are chosen out of the 110 simulation runs from the DOE in the same way as the previous case studies. The values of the decision variables and the NPV for the reference case and for the best overall solutions found by GA and PSO are presented in Table 4. The reference case for this case study gives a higher NPV than case studies 1 and 2. This is mainly due to a longer total WAG duration and a higher total oil production. Tables S7 and S8 in the Supplementary file present the global best solutions of each trial of GA and PSO, respectively. The values of the optimized variables which differ from the reference case have been marked with an asterisk.

Table 4 shows that GA always converges to a suboptimal solution and is never able to find the solution found by PSO in any of the trials. GA finds quite different values for the cycle time in the trials (see Table

Table 4
The reference case and best operational points found by GA and PSO (case study 3: NPV optimization over 13 variables).

Variable	Reference case	GA trial 2	PSO trials 1–4
Q _w (F-1H) [Sm ³ /day]	2700	2700	2700
Q _g (F-1H) [Sm ³ /day]	1000	1000	1000
Q _w (F-3H) [Sm ³ /day]	2700	2700	2700
Q _g (F-3H) [Sm ³ /day]	1000	1000	1000
BHP (E-2AH) [bar]	150	150	150
BHP (E-3CH) [bar]	150	150	150
BHP (E-3H) [bar]	150	237.5*	226.2*
Cycle ratio [–]	0.55	0.9*	0.9*
Cycle time [month]	2	7*	8*
Total time [month]	60	60	60
Mole fraction of C ₂ [–]	0.2	0.2	0.2
Mole fraction of C ₃ [–]	0.02	0.1*	0.1*
Mole fraction of C ₄ [–]	0.05	0.05	0.05
NPV [\$ million]	194.72	221.65	222.29

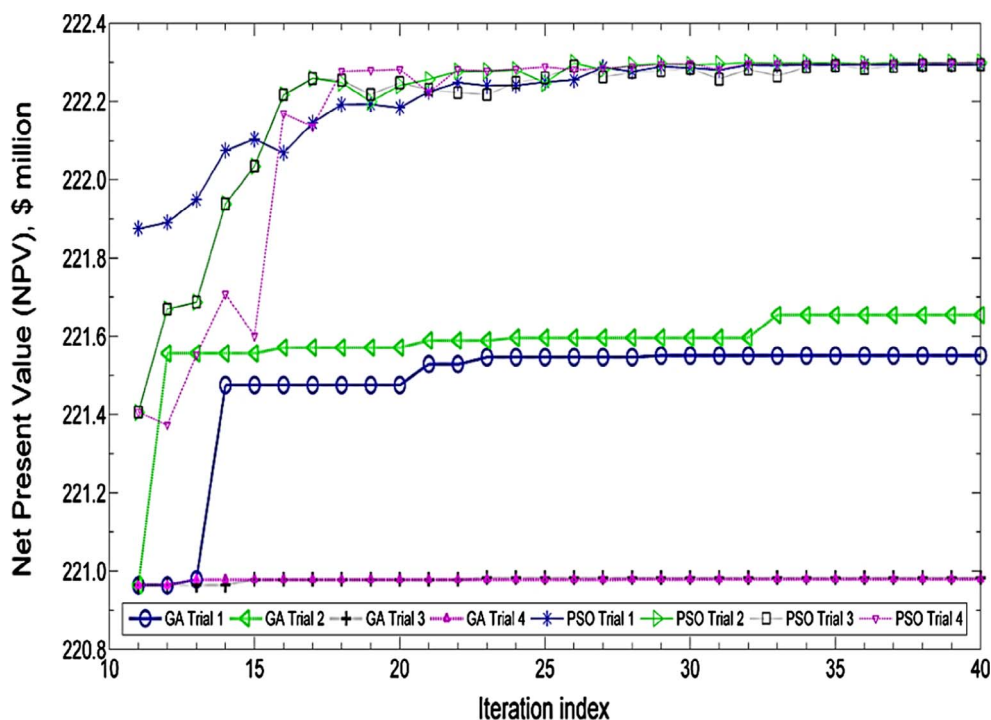


Fig. 4. NPV vs. iteration index per trial for iterations 11–40 of GA and PSO (case study 3: NPV optimization over 13 variables).

S7), neither of which yields the optimum NPV found by PSO. However, the best NPV found by PSO is only 0.29% higher than the optimal NPV of GA. This is due to different BHPs for well E-3H and different cycle times. The best NPV of GA is about 13.8% higher than the NPV value of the reference case. In the optimal solution found by PSO, the BHP of well E-3H increased from 150 bar to 226.2 bar, the cycle ratio changed from 0.55 to 0.9, the cycle time shifted from 2 months to 8 months and the mole fraction of C_3 changed from 0 to 0.1. This resulted in about 14.2% increase in NPV compared to the reference case. PSO converges to the same solution in all the trials.

The best NPVs of iterations 11–40 of all the trials of GA and PSO are plotted versus the iteration index in Fig. 4 and Fig. S4 in the Supplementary file shows the results of all the iterations per trial. The similar trend and behavior of the performance of GA and PSO as observed in the previous case studies can be drawn from the above figures.

PSO finds a solution with an NPV in the vicinity of 0.01% of the optimum solution for the first time in iteration 27, 22, 26 and 18 of trials 1–4, respectively. GA never finds such a point in any of the trials. It is difficult to isolate the effect of problem complexity on the rate of convergence of optimization techniques due to the effect of the initial guess. Nevertheless, PSO on average finds a solution in the vicinity of 0.01% of the optimal solution for the first time in iteration 7 of case study 1, iteration 20 of case study 2 and iteration 23 of case study 3. GA finds such an answer only in iteration 9 of one of the trials of case study 1.

The main difference between case study 3 and case studies 1 and 2 is the addition of the total time as a variable and setting 60 months as its upper bound. This has resulted in two major differences in the optimal operational points. In case studies 1 and 2, the optimal BHP of well E-2AH is about 158.8 bar and wells E-3CH and E-3H would give a higher NPV if produced at the lower pressure bound (150 bar). In case study 3, the optimal BHP of well E-2AH and E-3CH is the minimum (150 bar) and well E-3H would produce optimally at around 226.2 bar. The other distinction is the cycle time. The optimal cycle time of case studies 1 and 2 lies at 5 months, while it was found to be 8 months for case study 3. The optimal NPV of case study 3 (\$ 222.29 million) is about 51.7% and 49.4% higher in value compared to the optimal NPVs of case studies 1 (\$ 146.56 million) and 2 (\$ 148.76 million), respectively.

Fluctuations in the best NPV found by PSO versus the iteration index seem to be a feature of this PSO implementation, while GA has usually proved to be monotonically increasing in the value of the objective function. GA keeps the best ever solution and if the GA operations (selection, crossover and mutation) do not result in a better solution, the global best solution would be transferred to the next iteration. In PSO, however, the positions of all the particles are updated by a random factor of the position of the global best solution, hence the best found solution may not carry over to the next iteration. These fluctuations, however, probably help PSO escape from local optima.

5.4. NPV sensitivity studies

A sensitivity analysis is a means to measure the effect of independent parameters on the objective function. In this study, to examine the effect of an individual WAG operational parameter on NPV, all the other parameters are kept constant at their optimal values. The normalized NPV (the ratio of NPV to the maximum NPV found by the optimization algorithms for case study 3) is plotted versus the normalized variables (the ratio of each variable to its optimal value). The trend and slope of each curve shows how that parameter affects the objective function.

Fig. 5(a) shows the effect of the BHPs of the producers on the NPV. The optimal BHP of well E-3H is about 226.2 bar. The normalized BHP of well E-3H is changed on the interval [0.8, 1.05] in steps of 0.05 for the sensitivity study. Setting the BHP below the optimal value delays and reduces water production and enhances the NPV, while setting it above the optimal value causes the oil production to fall below the economic limit. The optimal BHP of wells E-2AH and E-3CH is 150 bar. The normalized BHPs of these two wells are changed on the interval [1.05, 1.2] in steps of 0.05 for the sensitivity analysis. These two wells behave normally in the sense that by increasing the BHP the oil production reduces significantly which affects the NPV. This indicates that well E-3H is the most sensitive well to water production.

The effect of cycle ratio on NPV is presented in Fig. 5(b). The optimal cycle ratio is 0.9 which means that in each cycle water is injected for 90% of the time and the rest is allocated to gas injection. It is worth recalling that cycle ratio was changed in steps of 0.05 through the

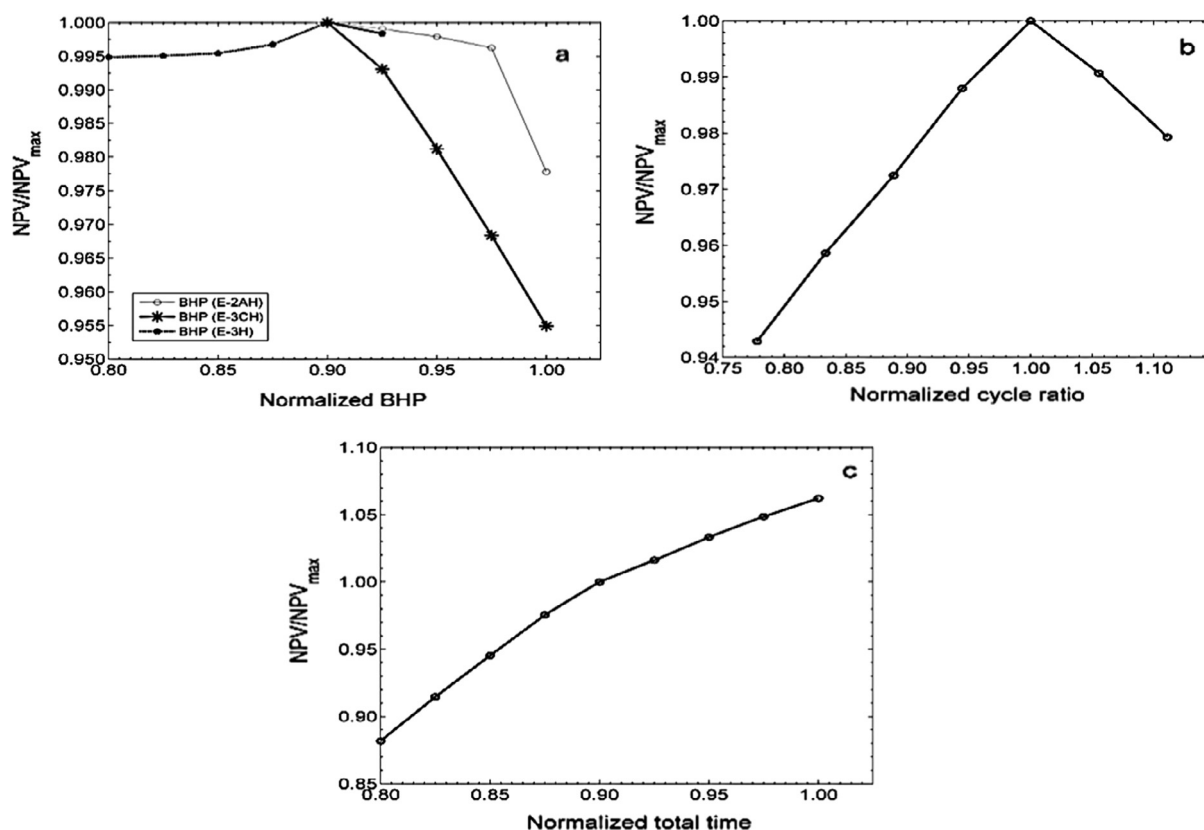


Fig. 5. (a) Effect of BHP on the NPV. (b) Effect of cycle ratio on the NPV. (c) Effect of total WAG time on the NPV.

search process of the optimization. For the sensitivity analysis, this parameter was changed from 0.7 to 1 in steps of 0.05. A cycle ratio of 1 refers to water flood. As can be seen, for a cycle ratio less than 0.9 (when gas is injected for more than 10% of a cycle), the NPV is lower than the optimum. This implies that increasing the gas injection period above that threshold does not result in enough oil production to make up for the cost of gas injection. When water is injected for more than 90% of a cycle the cost of water handling reduces the NPV below the optimum. The optimal cycle ratio depends strongly on the prices assumed for the NPV calculations. The optimal cycle time for the 5-year WAG process is 8 months. This means that the most economically efficient WAG injection scenario for a period of 5 years is to inject gas for 24 days and then inject water for 216 days (based on the cycle ratio of 0.9), cyclically.

The effect of the total WAG time is shown in Fig. 5(c). The normalized total time is changed on the interval [0.8, 1.2] in steps of 0.05. As shown, the NPV is strictly increasing versus the total WAG time. This suggests that WAG has the potential of being extended for at least one more year and would still be economical. However, the optimal operational WAG parameters for the 5-year period may not result in the highest NPV for a longer period and the optimal WAG for a longer period would have to be determined in a separate optimization process.

5.4.1. Sensitivity analysis of economic parameters

The economic parameters of oil price, gas injection cost, water injection cost and water recycling cost are selected for the sensitivity study to investigate their effect on the NPV. The injection and operating costs are all included in the assumed prices. When the effect of one economic parameter on NPV is examined, the other parameters are set at the values shown in Table S2. The gas injection cost is \$0.271 / Sm³ which is the unit price of gas containing 65% C₁, 20% C₂, 10% C₃ and 5% C₄, each of which costs the price assumed in Table S2. Fig. S5 shows the ratio of NPV to the best overall NPV found in case study 3 versus the normalized prices (the ratio of each price to its corresponding value in

Table S2). The normalized oil price is varied on the interval [0.8, 1.2] in steps of 0.05. The other normalized prices are changed on the interval [0, 1.2] to test the assumption of zero cost for injection and recycling.

As shown in Fig. S5, the relative change of NPV versus the relative change of the economic parameters clearly indicates that the NPV of WAG changes significantly as the oil price varies and oil price is the most influential economic parameter on the NPV. Water recycling cost has the second highest effect on the NPV and gas injection and water injection costs are ranked third and fourth, respectively. The effects of gas and water injection costs are much smaller than that of oil price and this is indicated by smaller slopes (in absolute value).

5.5. Case study 4: IRF optimization

In this section, GA and PSO are employed to optimize the incremental recovery factor (IRF) or the recovery factor from the start of the WAG, on the E-segment of the Norne field. The optimization variables include two water and two gas injection rates, three BHPs of the oil producers, cycle ratio, cycle time and the mole fractions of C₂, C₃ and C₄. The total WAG time is fixed at 60 months. The top 50 results out of the 96 simulation runs from the DOE are used as the initial positions for the 50 particles in PSO and the 50 members of the population for the GA optimization and the best of the 50 (the one with the maximum oil recovery) is chosen as the reference case for comparison.

Three trials of GA and PSO (six trials in total) with the same initial guess are run. The variables along with their values and the IRF calculated from the start of the WAG (as time zero) for the reference case and the best operational points found by GA and PSO are shown in Table 5. The best solution of each trial of GA and PSO are presented in Tables S9 and S10 in the Supplementary document. The values of the optimized variables which differ from the reference case have been marked with an asterisk.

As shown in Table 5, PSO converged to the same optimal solution in all the three trials. In the best solution found by PSO, the values of the

Table 5
The reference case and best operational points found by GA and PSO (oil recovery optimization).

Variable	Reference case	GA trial 2	PSO trials 1–3
Q _w (F-1H) [Sm ³ /day]	500	2700*	2700*
Q _g (F-1H) [Sm ³ /day]	10 ⁶	10 ⁶	10 ⁶
Q _w (F-3H) [Sm ³ /day]	500	2700*	2700*
Q _g (F-3H) [Sm ³ /day]	10 ⁶	10 ⁶	10 ⁶
BHP (E-2AH) [bar]	150	150	150
BHP (E-3CH) [bar]	150	150	150
BHP (E-3H) [bar]	240	237.5*	209*
Cycle ratio [–]	0.1	0.1	0.15*
Cycle time [month]	2	8*	12*
Mole fraction of C ₂ [–]	0.2	0.2	0.2
Mole fraction of C ₃ [–]	0.1	0.1	0.1
Mole fraction of C ₄ [–]	0.01	0.05*	0.05*
IRF [–]	4.45%	5.08%	5.17%

variables for the reference case changed as follows. The water injection rates increased to their maximum value, the BHP of well E-3H decreased from 240 bar to 209 bar, the cycle ratio changed from 0.1 to 0.15, the cycle time shifted from 2 months to 12 months and the mole fraction of C₄ increased to 0.05. This resulted in about 16.2% increase in the IRF compared to the reference case. GA is not able to find the optimal set of BHPs and the optimal cycle ratio found by PSO and reduces one of the gas injection rates to a non-optimal value in one of the trials (see Table S9). GA finds quite different solutions in the three trials, the best of which is about 14.2% higher than the reference case IRF.

The maximum IRFs of iterations 11–40 of the individual trials of GA and PSO and the best results of all the iterations are plotted versus the iteration index and shown in Fig. 6 and Fig. S6, respectively. The main observations in the performance of the optimization techniques are similar to the previous case studies.

PSO finds a solution with an IRF in the vicinity of 0.01% of the optimal solution for the first time in iteration 28 in all three trials. GA never finds a solution in the specified range in any of the trials.

Fig. 7 shows the optimal IRF for each simulation run among the three trials of GA and PSO. The amplitude of fluctuations in the GA solutions is higher than that of PSO and GA usually yields a lower recovery factor.

The optimal water injection rates are the same (2700 Sm³/day) for both NPV and IRF optimization, however, the optimal gas injection rates are set at the lower bound (1000 Sm³/day) for NPV optimization and at the upper bound (1,000,000 Sm³/day) for IRF optimization. When there is no restriction on the injection rates from the point of view of economic benefit (in the case of IRF optimization), a higher injection rate would probably result in more oil production.

The optimal BHP of well E-3H is a little different for NPV optimization (226.2 bar) and oil recovery optimization (209 bar) due to the relative prices of oil and water handling. As expected, a lower BHP results in more oil production and the difference in the BHPs indicates the sensitivity of well E-3H to water production.

The optimal cycle ratio for oil recovery optimization is 0.15 which means that in each cycle water is injected for 15% of the time and the rest is allocated to gas injection. The optimal cycle ratio for NPV optimization is 0.9 which means that longer periods of water injection are more beneficial from economic point of view, however, an optimum of 0.15 for the case of IRF optimization indicates the greater effect of longer periods of gas injection on the oil recovery.

12 months yields the highest oil recovery as the optimal cycle time for a 5-year WAG process. This means that the most efficient WAG injection scenario to produce the most oil in a 5-year period is to inject gas for 306 days and then inject water for 24 days (based on the cycle ratio of 0.15) cyclically. The optimal cycle time for case study 3 is 8 months. This indicates that if more oil recovery is required then less alternation between gas and water injection is necessary.

The most enriched injection gas composition (65% C₁, 20% C₂, 10% C₃ and 5% C₄) is the optimal solution for the case studies of NPV and IRF optimization. This means that with the assumed prices, the richest injection gas yields the greatest oil recovery as well as the greatest economic benefit.

The oil recovery factors from different recovery methods are presented in Fig. 8 from the start of the WAG project to the end of the 5-

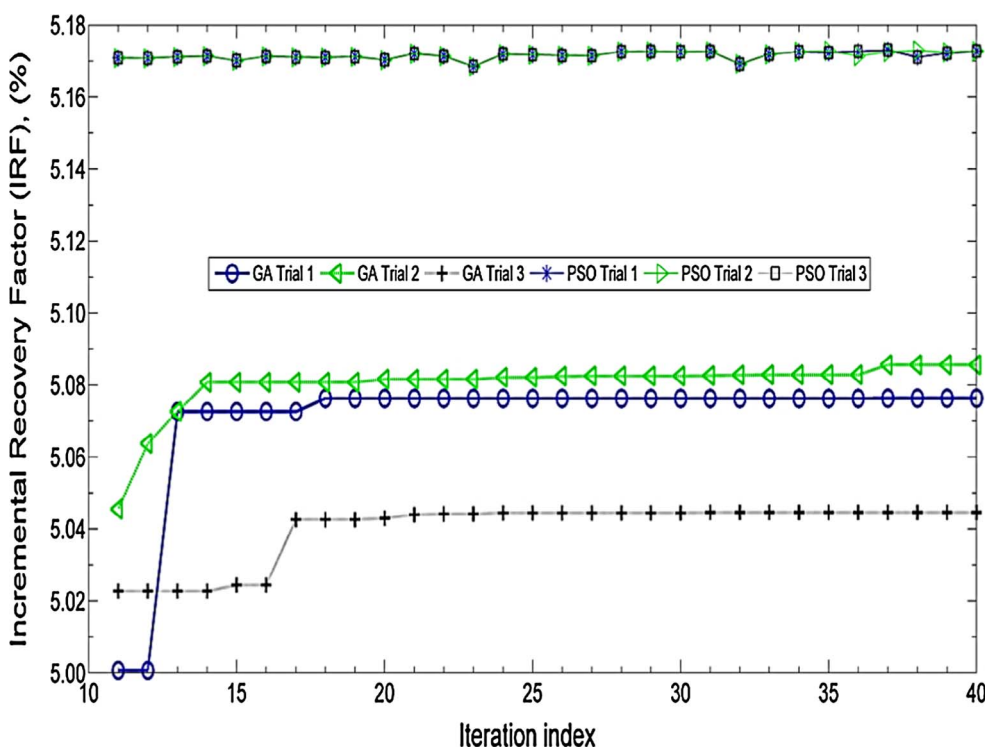


Fig. 6. IRF vs. iteration index per trial for iterations 11–40 of GA and PSO (oil recovery optimization).

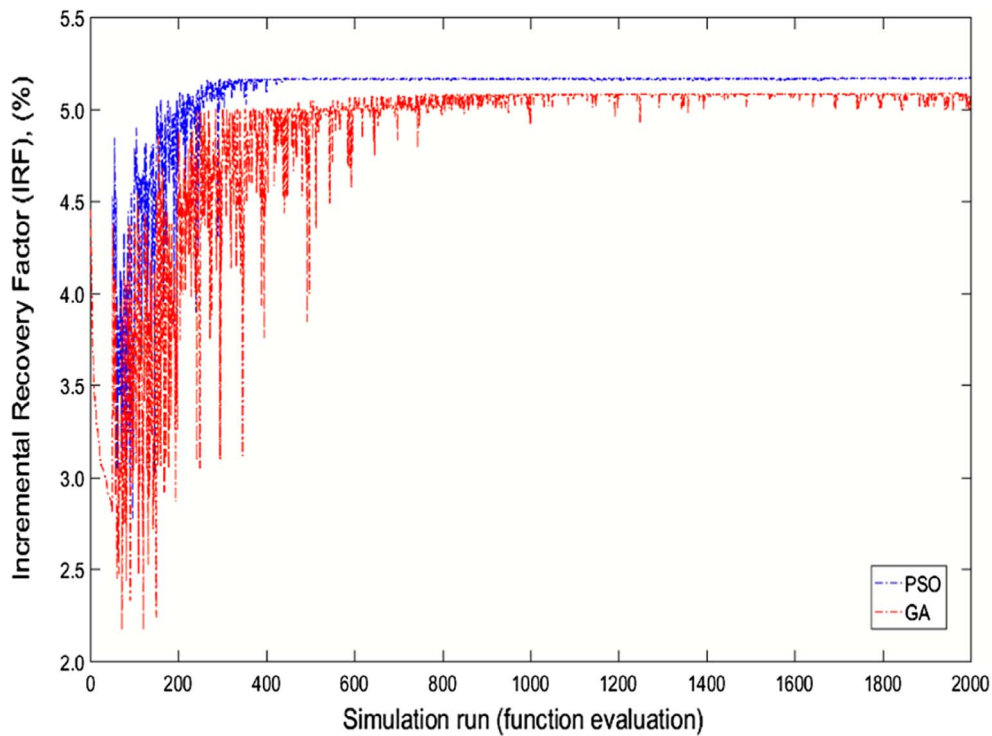


Fig. 7. IRF of the best solution as a function of simulation run for PSO (blue curve) and GA (red curve). (For interpretation of the references to colour in this figure legend, the reader is referred to the web version of this article.)

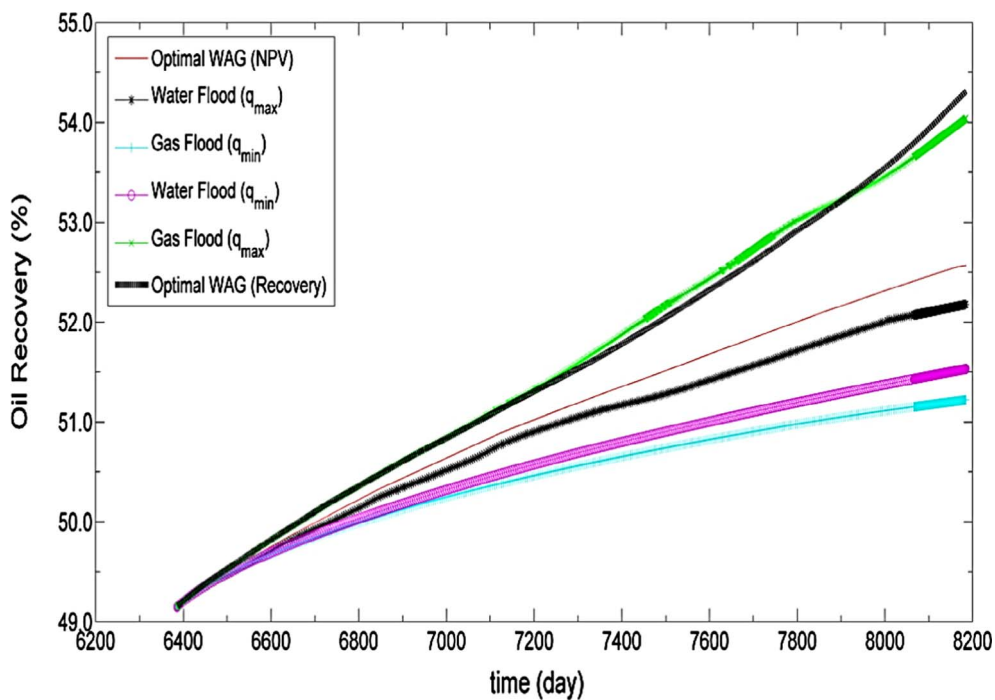


Fig. 8. Comparison of the oil recovery among different recovery methods.

year period. The recovery methods under investigation include the optimal WAG (from the viewpoint of NPV), water flooding with minimum and maximum injection rates, gas flooding with minimum and maximum injection rates and optimal WAG (from the viewpoint of oil recovery). The oil recovery at the start of the project is about 49.15%. The ultimate recoveries are as follows: 54.31% for the optimized-recovery WAG, 54.04% for gas flooding with the maximum injection rate (1,000,000 Sm³/day), 52.57% for the optimized-NPV WAG, 52.17% for water flooding with the maximum injection rate (2700 Sm³/

day), 51.53% for water flooding with the minimum injection rate (500 Sm³/day) and 51.22% for gas flooding with the minimum injection rate (1000 Sm³/day). The optimized-NPV WAG process is ranked third after the optimized-recovery WAG and gas flooding with the maximum injection rate. Continuous gas flooding with the minimum injection rate yields the lowest recovery.

The cumulative production and injection data (see Table S11) and the NPV calculation for the WAG scenario yielding the maximum oil recovery are shown in the Supplementary file. The huge negative NPV

(\$532 million) for this case clearly indicates the lack of any economic justification for increasing the gas injection rate and period.

6. Conclusions

Two evolutionary algorithms, a genetic algorithm (GA) and particle swarm optimization (PSO) were utilized to develop an optimization methodology and determine the optimal water alternating gas (WAG) operating parameters in a natural gas WAG process simulated using Schlumberger's compositional Eclipse 300. The full set of optimization variables consists of water and gas injection rates, bottom hole pressures of the production wells, cycle ratio, cycle time, the total WAG time, and the composition of the injection gas. A reference case was first obtained for each case study by means of DOE and then both GA and PSO were applied and compared to the base case. Three case studies to optimize NPV with different numbers of controlling variables (9, 12 and 13) and one case study to optimize incremental oil recovery (with 12 variables and a fixed total WAG time) were analyzed.

Both of the optimization techniques were capable of improving the values of the objective functions (NPV and incremental oil recovery) compared to the reference case. They were able to find a reasonable solution over all the variables using 2000 objective function evaluations, while an exhaustive search over only the discrete variables (the cycle ratio, cycle time and total WAG duration) required more than 7000 objective function evaluations. The differences in the values of the optimal solutions found by the algorithms were small. PSO converged to the same optimal solution in all the trials for each case study and marginally outperformed GA. GA usually converged to different solutions in different trials of the same case study and yielded an inferior solution. Further tuning of GA and PSO would help us draw a stronger conclusion.

As the number of WAG operating parameters increases, the optimization techniques, especially PSO, were able to find a higher NPV but generally required more iterations.

Acknowledgements

The authors would like to thank Chevron Canada, Hibernia Management and Development Company (HMDC), Petroleum Research Newfoundland and Labrador (PRNL), Innovate NL, and the Natural Sciences and Engineering Research Council of Canada (NSERC) for their financial support of this research.

Appendix A. Supplementary data

Supplementary data associated with this article can be found, in the online version, at <http://dx.doi.org/10.1016/j.fuel.2018.01.138>.

References

- [1] Lake LW. *Enhanced oil recovery*. Englewood Cliffs, NJ: Prentice Hall; 1989.
- [2] Green DW, Willhite GP. *Enhanced oil recovery*. Richardson, Tex.: Henry L. Doherty Memorial Fund of AIME, Society of Petroleum Engineers; 1998.
- [3] Ampomah W, Balch R, Cather M, Will R, Gunda D, Dai Z, et al. Optimum design of CO₂ storage and oil recovery under geological uncertainty. *Appl Energy* 2017;195:80–92.
- [4] Dai Z, Viswanathan H, Middleton R, Pan F, Ampomah W, Yang C, et al. CO₂ accounting and risk analysis for CO₂ sequestration at enhanced oil recovery sites. *Environ Sci Technol* 2016;50(14):7546–54.
- [5] Ampomah W, Balch RS, Grigg RB, McPherson B, Will RA, Lee SY, et al. Co-optimization of CO₂-EOR and storage processes in mature oil reservoirs. *Greenhouse Gases Sci Technol* 2016.
- [6] Soltanian MR, Amooie MA, Dai Z, Cole D, Moortgat J. Critical dynamics of gravito-convective mixing in geological carbon sequestration. *Sci Rep* 2016;6.
- [7] Kulkarni MM, Rao DN. Experimental investigation of miscible and immiscible Water-Alternating-Gas (WAG) process performance. *J Petrol Sci Eng* 2005;48(1):1–20.
- [8] Hagoort J. Oil recovery by gravity drainage. *Soc Petrol Eng J* 1980;20(03):139–50.
- [9] Christensen JR, Stenby EH, Skauge A. Review of WAG field experience. *SPE Reservoir Eval Eng* 2001;4(02):97–106.
- [10] Hemmati-Sarapardeh A, Ayatollahi S, Zolghadr A, Ghazanfari M-H, Masihi M. Experimental determination of equilibrium interfacial tension for nitrogen-crude oil during the gas injection process: the role of temperature, pressure, and composition. *J Chem Eng Data* 2014;59(11):3461–9.
- [11] Fathinasab M, Ayatollahi S, Hemmati-Sarapardeh A. A rigorous approach to predict nitrogen-crude oil minimum miscibility pressure of pure and nitrogen mixtures. *Fluid Phase Equilib* 2015;399:30–9.
- [12] Quijada MG. *Optimization of a CO₂ flood design Wesson Field-west Texas* [Master Thesis]. Texas A&M University; 2005.
- [13] Ma J. *Design of an effective water-alternating-gas (WAG) injection process using artificial expert systems*. The Pennsylvania State University; 2010.
- [14] Chen S, Li H, Yang D, Tontiwachwuthikul P. Optimal parametric design for water-alternating-gas (WAG) process in a CO₂-miscible flooding reservoir. *J Can Pet Technol* 2010;49(10):75–82.
- [15] Rogers JD, Grigg RB. A literature analysis of the WAG injectivity abnormalities in the CO₂ process. *SPE/DOE Improved Oil Recovery Symposium*. Society of Petroleum Engineers; 2000.
- [16] Song Z, Li Z, Wei M, Lai F, Bai B. Sensitivity analysis of water-alternating-CO₂ flooding for enhanced oil recovery in high water cut oil reservoirs. *Comput Fluids* 2014;99:93–103.
- [17] Mollaei A, Delshad M. A Novel Forecasting Tool for Water Alternating Gas (WAG) Floods. *SPE Eastern Regional Meeting*. Society of Petroleum Engineers; 2011.
- [18] Attanucci V, Aslesen K, Hejl K, Wright C. WAG process optimization in the Rangely CO₂ miscible flood. In: *SPE Annual Technical Conference and Exhibition*. Society of Petroleum Engineers; 1993.
- [19] Guo X, Du Z, Sun L, Huang W, Zhang C. Optimization of tertiary water-alternate-CO₂ flood in Jilin oil field of China: Laboratory and simulation studies. *SPE/DOE Symposium on Improved Oil Recovery*. Society of Petroleum Engineers; 2006.
- [20] Hallam RJ, Ma TD, Reinbold EW. Performance evaluation and optimization of the Kuparuk hydrocarbon miscible water-alternating-gas flood. *Geological Society, London, Special Publications* 1995;84(1):153–64.
- [21] Pritchard D, Nieman R. Improving oil recovery through WAG cycle optimization in a gravity-overide-dominated miscible flood. *SPE/DOE Enhanced Oil Recovery Symposium*. Society of Petroleum Engineers; 1992.
- [22] Ampomah W, Balch R, Cather M, Rose-Coss D, Dai Z, Heath J, et al. Evaluation of CO₂ storage mechanisms in CO₂ enhanced oil recovery sites: application to morrow sandstone reservoir. *Energy Fuels* 2016;30(10):8545–55.
- [23] Gharbi R. Application of an expert system to optimize reservoir performance. *J Petrol Sci Eng* 2005;49(3):261–73.
- [24] Esmaili TE, Heeremans JC. Optimization of the WAG process under Uncertainty in a Smart Wells Environment: Utility Theory Approach. *Intelligent Energy Conference and Exhibition*. Society of Petroleum Engineers; 2006.
- [25] Ghomian Y, Pope GA, Sepehrnoori K. Hysteresis and field-scale optimization of WAG injection for coupled CO₂-EOR and sequestration. *SPE Symposium on Improved Oil Recovery*. Society of Petroleum Engineers; 2008.
- [26] Ghaderi SM, Clarkson CR, Chen Y. Optimization of WAG Process for Coupled CO₂ EOR-Storage in Tight Oil Formations: An Experimental Design Approach. *SPE Canadian Unconventional Resources Conference*. Society of Petroleum Engineers; 2012.
- [27] Dai Z, Middleton R, Viswanathan H, Fessenden-Rahn J, Bauman J, Pawar R, et al. An integrated framework for optimizing CO₂ sequestration and enhanced oil recovery. *Environ Sci Technol Lett* 2013;1(1):49–54.
- [28] Dai Z, Viswanathan H, Xiao T, Middleton R, Pan F, Ampomah W, et al. CO₂ Sequestration and enhanced oil recovery at depleted Oil/Gas reservoirs. *Energy Procedia* 2017;114:6957–67.
- [29] Rahmawati SD, Whitson CH, Foss B. A mixed-integer non-linear problem formulation for miscible WAG injection. *J Petrol Sci Eng* 2013;109:164–76.
- [30] Jahangiri HR. Optimization of coupled CO₂ sequestration and enhanced oil recovery. University of Southern California; 2012.
- [31] Yang D, Zhang Q, Cui H, Feng H, Li L. Optimization of Multivariate Production-Injection System for Water-Alternating-Gas Miscible Flooding in Pubei Oil Field. *Society of Petroleum Engineers*; 2000.
- [32] Yang D, Zhang Q, Gu Y. Integrated optimization and control of the production-injection operation systems for hydrocarbon reservoirs. *J Petrol Sci Eng* 2003;37(1):69–81.
- [33] Harding T, Radcliffe N, King P. Hydrocarbon production scheduling with genetic algorithms. *SPE J* 1998;3(02):99–107.
- [34] Humphries TD, Haynes RD, James LA. Simultaneous and sequential approaches to joint optimization of well placement and control. *Comput Geosci* 2013;1:1–16.
- [35] Karkevandi-Talkhooncheh A, Hajirezaie S, Hemmati-Sarapardeh A, Husein MM, Karan K, Sharifi M. Application of adaptive neuro fuzzy interface system optimized with evolutionary algorithms for modeling CO₂-crude oil minimum miscibility pressure. *Fuel* 2017;205:34–45.
- [36] Montgomery DC. *Design and analysis of experiments*. John Wiley & Sons; 2008.
- [37] Chow C, Aronidin M. Managing risks using integrated production models: process description. *J Petrol Technol* 2000;52(03):54–7.
- [38] Naseri A, GhareSheikhloo AA, Kamari A, Hemmati-Sarapardeh A, Mohammadi AH. Experimental measurement of equilibrium interfacial tension of enriched miscible gas-crude oil systems. *J Mol Liq* 2015;211:63–70.
- [39] Holland JH. *Adaptation in natural and artificial systems: an introductory analysis with applications to biology, control, and artificial intelligence*. U Michigan Press; 1975.
- [40] Michalawicz Z. *Genetic algorithms + data structures = evolution programs*. Berlin: Springer-Verlag; 1997.
- [41] Chen G, Fu K, Liang Z, Sema T, Li C, Tontiwachwuthikul P, et al. The genetic algorithm based back propagation neural network for MMP prediction in CO₂-EOR

- process. *Fuel* 2014;126:202–12.
- [42] Velez-Langs O. Genetic algorithms in oil industry: an overview. *J Petrol Sci Eng* 2005;47(1):15–22.
- [43] The MathWorks Inc. MATLAB Global Optimization Toolbox Release 2016a. Massachusetts, United States; 2016.
- [44] Eberhart RC, Kennedy J. A new optimizer using particle swarm theory. Proceedings of the sixth international symposium on micro machine and human science. 1. New York, NY; 1995: p. 39–43.
- [45] Ahmadi MA, Shadizadeh SR. New approach for prediction of asphaltene precipitation due to natural depletion by using evolutionary algorithm concept. *Fuel* 2012;102:716–23.
- [46] Shi Y, Eberhart R. A modified particle swarm optimizer. Evolutionary Computation Proceedings, 1998. IEEE World Congress on Computational Intelligence., The 1998 IEEE International Conference on. IEEE; 1998. p. 69–73.
- [47] Perez R, Behdinan K. Particle swarm approach for structural design optimization. *Comput Struct* 2007;85(19):1579–88.
- [48] Bansal J, Singh P, Saraswat M, Verma A, Jadon SS, Abraham A. Inertia weight strategies in particle swarm optimization. Nature and Biologically Inspired Computing (NaBIC), 2011 Third World Congress on. IEEE; 2011: p. 633–40.
- [49] Cai X, Zeng J, Tan Y, Cui Z. Individual parameter selection strategy for particle swarm optimization. INTECH Open Access Publisher; 2009.
- [50] Schlumberger. ECLIPSE Compositional Simulation; 2010. Available from: <https://www.software.slb.com/products/eclipse/simulators>.
- [51] Statoil. PL128 Norne Field Reservoir Management Plan. 2001.
- [52] Nangacovié HLM. Application of WAG and SWAG injection Techniques in Norne E-Segment [Master Thesis]. Norwegian University of Science and Technology, Department of Petroleum Engineering and Applied Geophysics; 2012.
- [53] Harmon R, Grigg R. Vapor-density measurement for estimating minimum miscibility pressure (includes associated papers 19118 and 19500). *SPE Reservoir Eng* 1988;3(4):1215–20.
- [54] IO-Center-NTNU. Norne Field (E-segment) Case Description. 2008.
- [55] Chiyenne C. Enhanced Oil Recovery for Norne field's E-segment using surfactant flooding [Master Thesis]. Norwegian University of Science and Technology, Department of Petroleum Engineering and Applied Geophysics; 2010.
- [56] Amirbayov T. Simulation Study of the Polymer Flooding Applied to the Norne Field E-Segment [Master Thesis]. Norwegian University of Science and Technology, Department of Petroleum Engineering and Applied Geophysics; 2014.
- [57] Tveit M. A Comparative Simulation Study of Chemical EOR Methods Applied to the Norne E-Segment Using Eclipse 100. [Master Thesis]. Norwegian University of Science and Technology, Department of Petroleum Engineering and Applied Geophysics; 2014.
- [58] Chen S. Constrained Particle Swarm Optimization, Version 20140330. <http://www.mathworks.com/matlabcentral/fileexchange/25986>; 2009.